DEVELOPMENT OF FINITE ELEMENT ANALYSIS PROGRAM FOR ROTORDYNAMIC PREDICTION OF SINGLE AND MULTI-DISK ROTOR MODEL

MUHAMMAD IDRIS*, ZAKIE ANUGIA, DONNY MUSTIKA

PT PLN (Persero), Engineering and Technology Division, Jakarta, Indonesia

**Corresponding author: muhammad.idris@pln.co.id*

(Received: 13 July 2022; Accepted: 2 October 2022; Published on-line: 01 November 2022)

ABSTRACT: The rotating equipment is a crucial part of system performance reliability. Vibration, as a characteristic of an oscillating body, is a fundamental parameter to determine the dynamic behaviour of the rotor system. The dynamic characteristics include natural frequency, critical speed, mode shape, and vibration response. This paper discussed the application of rotordynamics analysis as a tool to numerically predict the dynamic behaviour of a rotor system. The aim is to determine a rotor system's natural frequency and critical speed by a finite element analysis (FEA) program. The selected method is validated using various analytical methods from other references with small discrepancies in the result. The calculation of FEA using the computational program; they applied the developed program to describe the dynamic characteristic of single and multi-disk rotors. The developed works provided comprehensive results about a rotor system's natural frequency, mode shape, and critical speed and predicted the vibration response due to unbalance. However, other types of rotors, such as coaxial dual rotors, can be further investigated to make the program capable of the general purpose of the rotor. Validation with the real case problem could be an interesting investigation to satisfy the result of developed works.

KEY WORDS: Rotordynamic, Vibration, critical speed, natural frequency, FEA

1. INTRODUCTION

Rotating equipment or rotor is one of the vital components of mechanical systems extensively used in power plants and industrial applications. It is fundamental to understand the dynamics characteristic of the rotor. The rotor shall be designed prudently considering the dynamic characteristics, such as vibration. Matsushita et al. [1] investigated the problematic mode in some rotating equipment. The investigation showed rotating equipment was commonly associated with vibration phenomena. An early examination of these causes would be necessary for the continuity of the operational assets. Knowing the characteristic of dynamic behavior of rotating equipment becomes a crucial issue in investigating the cause of vibration [2]. The rotor becomes a hazardous operational condition if it becomes unstable in the dynamic condition because of vibration. Hence, to prevent this dangerous condition is to cut off the vibration source by investigating the main problem, such as unbalance, misalignment, and improper design. It is required to know the rotordynamic characteristics in the operation and maintenance phases and the design stage [1].

Rotordynamic is a branch of applied mechanics focusing on the rotating equipment's dynamic and stability. It plays a significant role in the rotating systems' design, performance, and safety [3], [4]. In the rotating equipment design, predicting the rotors' dynamic behavior becomes a crucial step. Pumps, compressors, turbines, engines, propellers, motors, and blowers

are rotating equipment widely used in mechanical equipment. Rotordynamic is close relation to vibration study. Thus, rotordynamic describes vibration behavior in rotating machinery as well. The purposes of a rotordynamic analysis are to: investigate natural frequencies; predict the maximum amplitudes of vibration; estimate mechanical impedances such as stiffness, damping, and inertia force coefficients; predict rotordynamic instability (the damped natural frequencies and damping ratios); improve the rotor system performance such as stability and response [5]–[9]. The designing, operating, and maintaining rotating equipment, it is necessary to understand the causes of vibration, their mechanisms, and the natural frequencies [1].

To model the rotor problems, commonly, the one-dimensional model is the basic method of rotordynamic analysis referred to as the "Laval" or "Jeffcott" rotor model. It comprises beam-mass-spring elements for torsional and lateral vibration. Before 1883, the fundamentals of rotordynamics were not yet completely understood. Then Laval built the first impulse turbine. It was the first attempt to investigate the 1-DOF vibrating system for a rotor. Therefore, 1-disk rotor model is referred to Laval Rotors. Afterwards, many researchers discussed and developed Laval's fundamentals of rotordynamics. In 1919, Jeffcott formulated the rotor problem and significantly understood rotordynamic behavior. Jeffcott modeled the rotor as a single disk on a flexible shaft. It was like to 1-DOF mass-spring model which named as Jeffcott rotor model [10]. In 1924, Stodola presented the gyroscopic effects on a rotating system [10]–[12]. The computational program for rotordynamics has been developed to solve the rotordynamic model by using the tabular method [13], transfer matrix method [14] and finite element analysis (FEA) [15], [16]. Recent trends in rotordynamics analysis show the using FEA is one of the main tool to simulate the rotor. The application of the FEA is a valuable and important tool when the classic theory is difficult to apply and less costly and time-consuming than experimental analysis. Many FEA programs to solve various problems, such as ANSYS, COMSOL, DYNAMICS R4, DYNROT, MADYN, ROSS, RoViLab, ROTORINSA, XLTRC2 [17]–[23].

Rotordynamic investigations must accommodate vibration phenomena. The significant case in rotating equipment is vibration. It took over 50% of problematic cases, and 29% were caused by unbalance [2]—Unbalance phenomena in a rotor result from an uneven distribution of mass, which causes the rotor vibration. Hence, the rotordynamic analysis describes the unbalance response as the dynamic characteristic. Even though the dynamic phenomena were dominated with unbalance problems, many researchers investigated the other phenomena to assess the other problematic case in the rotor system.

Over the years, rotordynamic analysis capabilities have developed according to the rotating equipment application. The program's rotordynamic analysis technology and rotor application have been developed to meet industry requirements. The rotordynamic was conducted by researchers to investigate many purposes, such as critical speed, bearings, seals, casing, blade, and stability of the rotor. Table 1 shows the list of the rotordynamic application to solve various problems in rotating systems, and FEA has become the most popular method. However, the experimental method is the main validation of the rotor phenomena. Besides conventional rotating equipment (as mentioned in Table 1), recent rotordynamic developments have also supported tiny rotational equipment, particularly for computer devices, such as hard disks, optical disks, and compact disks [1].

This paper presents a development of the FEA program of the rotor to solve the basic dynamic behavior for single and multi-disk rotors. The aim is to predict the natural frequency, mode shape, critical speed, and dynamic response. Even though many papers and software have discussed and developed the rotordynamic problems and solutions, it is necessary to know the deep inside of discussion and software by developing the program to make it fully

understand rotordynamic in theoretical and numerical as well. However, experimental analysis is important to validate the numerical result. Thus, this study intends to observe the capability of using a mathematical model to simulate Campbell diagram, response of a rotor using only limited data from the rotor system. If the numerical analysis is proven workable, this program will provide some benefit in supporting the decision-making in the design, operation, and maintenance of rotating machinery.

Table 1: Rotordynamic application in various rotating equipment investigation

Author (Reference)	Application	Method	Work Area
Taplak and Parlak [23]	Gas turbine	Numerical analysis (FEA)	The Campbell diagrams to determine critical speeds
Nässelqvist [11]	Hydropower turbine	Numerical analysis (FEA)	The dynamic properties of the bearings
Moore et al. [24]	Turbocompressor	Numerical analysis (FEA)	The dynamic effect of casing and foundation.
Tenali and Kadivendi [18]	Steam turbine	Numerical analysis (FEA)	Critical speeds and system stability
Pace et al. [25]	Multistage pump	Numerical (FEA) and experimental analysis	Impeller hydraulic forces in rotordynamics analysis, the potential of swirl breaks to improve rotor stability
Shuguo et al. [26]	Aero-engine	Numerical (FEA) and experimental analysis	The dynamic effects of structure, the external load on the rotor joints
Mohan et al. [27]	Steam turbine	Numerical analysis (FEA)	The flexural dynamics of turbine blades
Hirano et al. [28]	Steam turbine	Numerical analysis (FEA)	The assessment of unstable vibration due to the seal force (steam whirl)
Moore [29]	Centrifugal compressor	Numerical analysis (FEA)	Rotordynamic investigation for gas labyrinth seals
Sivaneri and Chopra [15]	Helicopter rotor blade	Numerical analysis (FEA)	The trim deflections of blades and the aero-elastic stability
Subramanian et al. [30]	Gas turbine	Numerical analysis (FEA)	The rotordynamic behavior of seals

2. MATERIALS AND METHODS

2.1. Methods

Numerical analysis is a very extensive application for investigating the dynamic behavior of rotating equipment. FEA has become the most popular method for examining the rotordynamic. In this study, numerical modeling with the FEA is carried out. Numerical modeling is governed by programming code. The numerical modeling result is validated analytically using the energy method and several references to ensure that the modeling is correct. The validation process is carried out with iterations of model improvement until the results are quite close.

Several parameters are simulated and then applied in the model; the one-dimensional rotor models are selected due to the practical needs of rotordynamics. The Campbell diagrams are very important in investigating the dynamic characteristic of rotors. Therefore, getting the Campbell diagrams of the rotating systems and determining the critical speeds are important for observing rotor system behaviors. The sequence of activities is described in the following flowchart, as shown in Fig. 1.

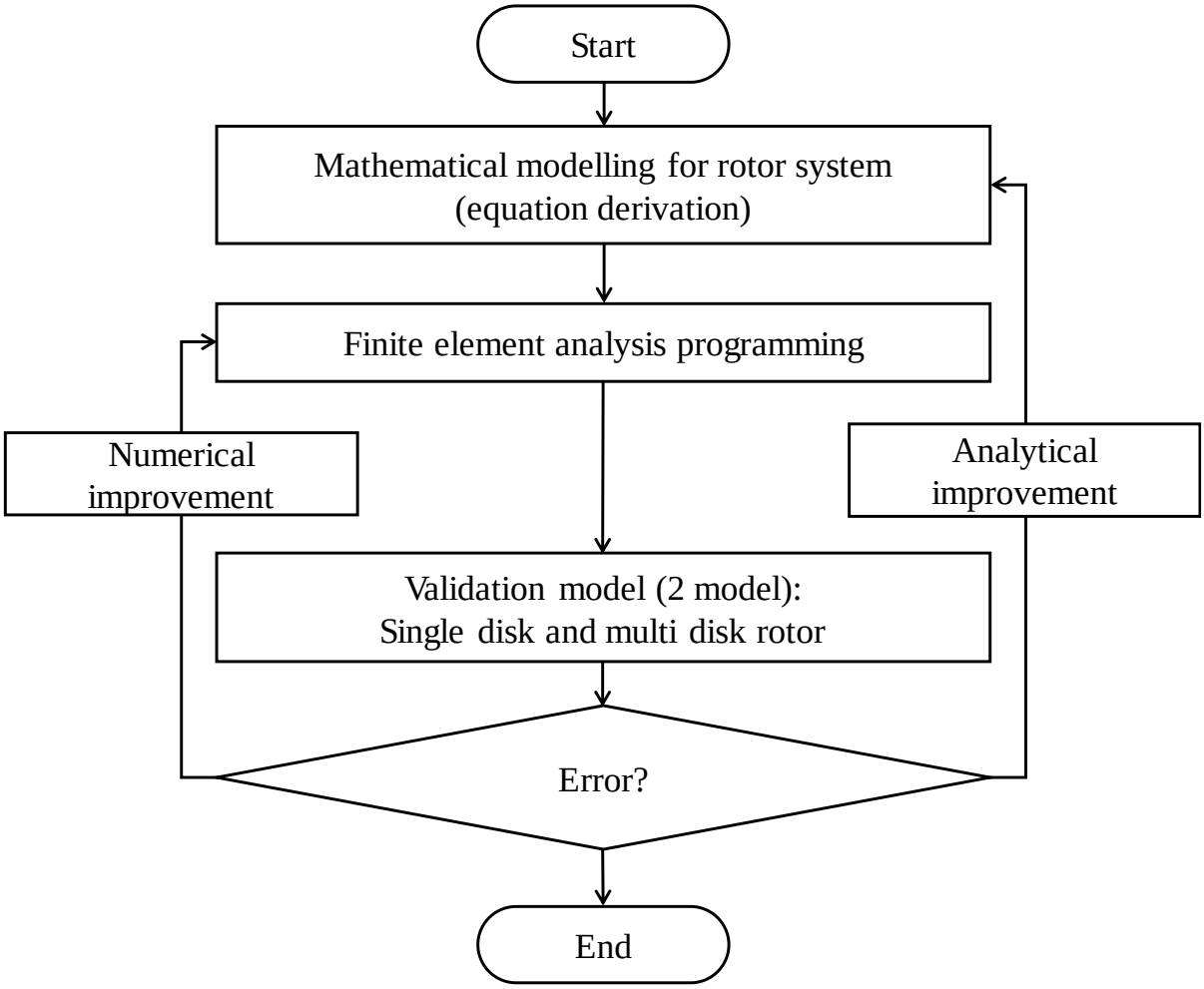

Fig. 1. Flowchart of method

2.1. Single Rotor and Multi-Disk Rotor Model

Model validation comprises a rotor with single disk (model 1) and a multi-disk (model 2). This simplified model is a justification that the derivation of the programming code is 'true'. A simple model is used to find the rotor system's frequency and critical speed. Fig. 2 shows the validation model for a single disk rotor. For the specific geometries and properties of rotor elements, see Fig. 2. Rotor comprises one disk supported by bearings. The disk is in node 3; both the model bearings by spring and damper elements have similar stiffness and coefficient damper. The bearing was in node 1 and node 4. The material of the shaft and disk is steel. The analytical method and FEA method as calculation models. The comparison parameter comprises natural frequency and critical speed. The natural frequency is compared to the calculation result by Lallane & Ferraris [3] and Gorman & Belvins [31] as verificatory. The calculation of natural frequency when the rotor was not rotating. In the analytical method, the assumption support model is to be supported (pin-roll) by the first displacement mode shape function. The FEA method divided the rotor into 3 elements (4 nodes). The calculation of the critical speed using the Campbell diagram. This case applies the analysis of 2 modes.

Fig. 3 shows the model for the multi-disk rotor. For the specific geometries and properties of rotor elements, see Fig. 3. The rotor divide becomes 13 elements (14 nodes). The rotor comprises 3 disks and is supported by bearings. The disks are in nodes 3, 6, and 11. The bearings are modeled by spring and damper elements with similar stiffness and coefficient

damper. The bearing was in node 1 and node 14. The material of the shaft and disk is steel. The comparison parameter comprises frequency at operational speed and critical speed. The frequency and critical speed compared to the calculation result by the Lallane & Ferraris [3]. The calculation of frequency when the rotor rotated at 25000 rpm and critical using the Campbell diagram. This model is analyzed for an 8-mode shape.

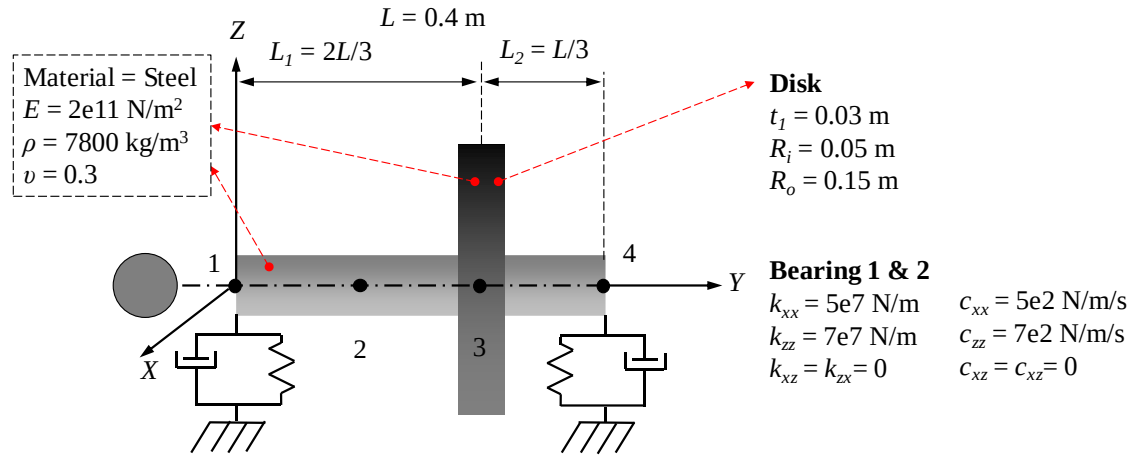

Fig. 2. Validation model 1 (rotor with single disk)

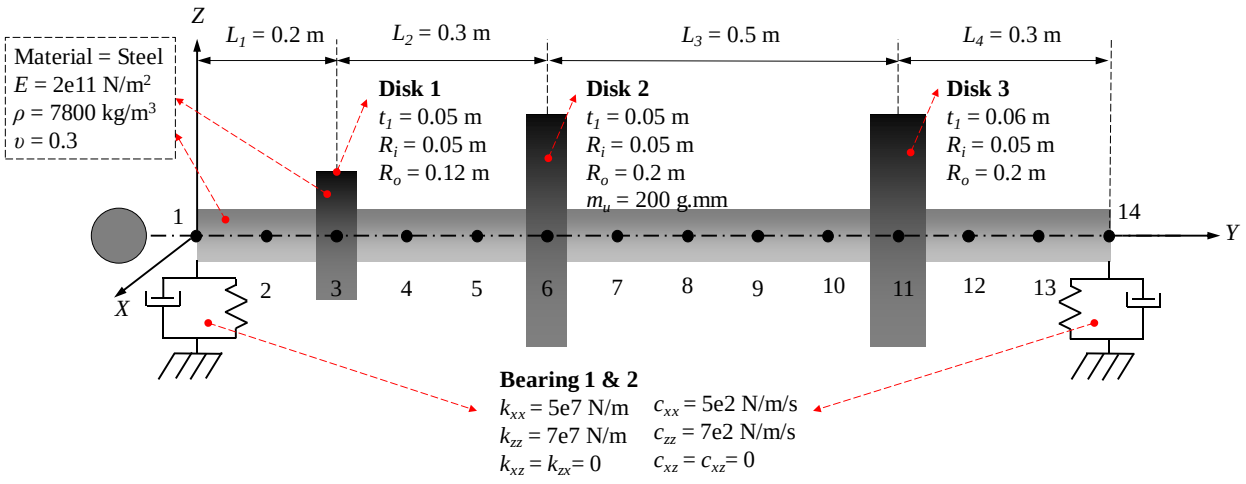

Fig. 3. Validation model 2 (rotor with multi-disk)

2.2. Solution Approach

The rotor is a rotating part of the machine or equipment that has functions to transmit the rotation. The basic elements in the rotor are the shaft, disk, bearing, and seal [3], [4], [31]. The shaft, disk, bearing, and seal contribute to the theoretical dynamics equations. In real applications, disks represent turbine blades, impeller wheels, propellers, fans, pulleys, gears, etc. The mass cannot be ignored and shall be considered in the rotor model. The general rotor equations comprise kinetic energy (T), strain energy (U), and forces (F). The disk, shaft, and mass unbalance expressed by T. The shaft is described by U. The forces due to the bearing and seal are used to calculate virtual work. Fig. 4 shows the rotor element and the energy equation

involved in the rotordynamic characteristic, such as kinetic energy, strain energy, and virtual works.

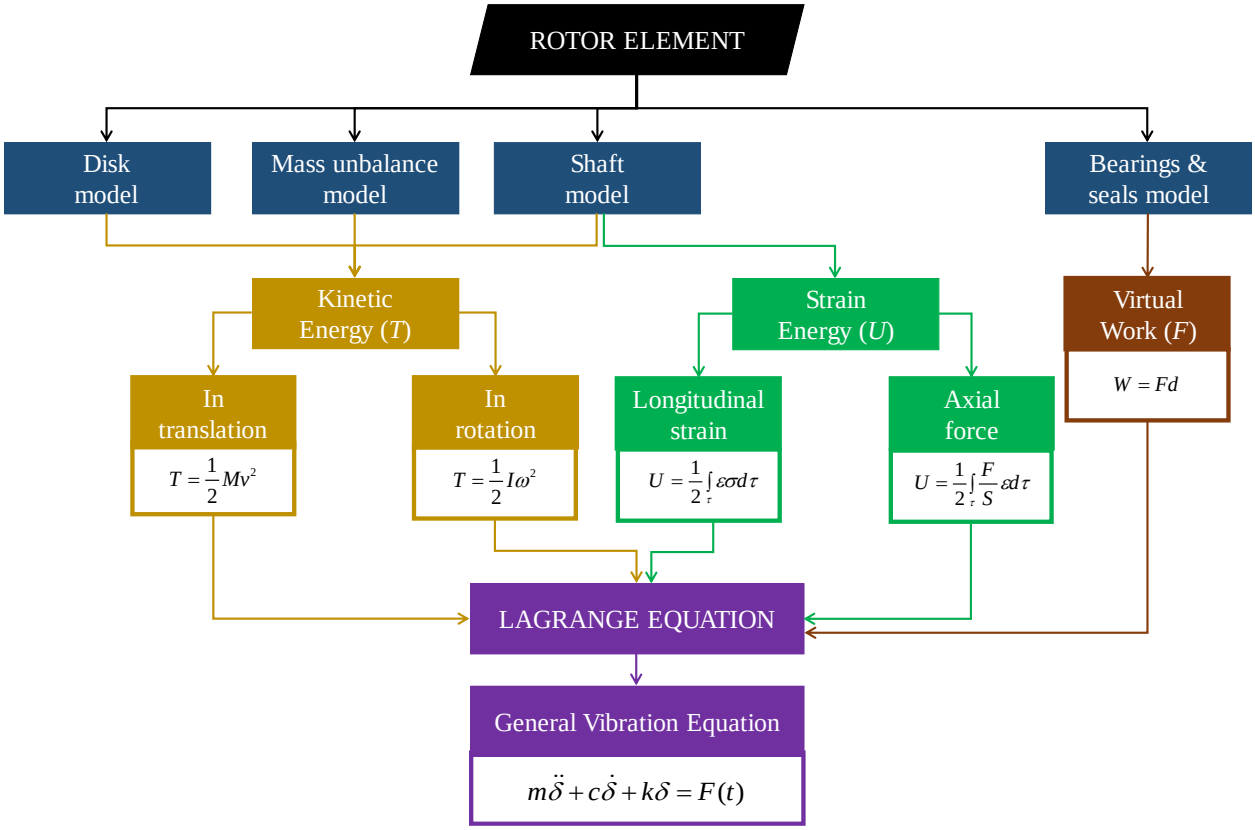

Fig. 4. Flowchart of solution approach to get general vibration equation

The rotor system is simplified and assumed to have the following scheme, as shown in Fig. 5(a). The rigid body is taken as an assumption for the disk and characterized by its kinetic energy. The *XYZ* coordinate is the initial frame reference. The $x_1y_1z_1$ coordinate is a frame reference due to the displacement of angle (θ) concerning *XYZ*. The *xyz* coordinate is a frame reference due to the displacement of angle (ϕ) concerning $x_1y_1z_1$. The $\dot{\theta}$, $\dot{\varphi}$, and $\dot{\psi}$ are the rotational speed in x_1, *y, and Z*-axis, respectively. The *u* and *w* are displacements in the *X* and *Z* direction, respectively. The rotational speed (Ω) of the shaft is $\dot{\varphi}$. The symbol of *u* and *w* are designated as displacement toward *X* and *Z*, respectively. Fig. 5(b)-(d) shows the schematic model of each rotor element, such as the shaft, bearings, and mass unbalance.

The Lagrange equation (Eq. (1)) is used to govern vibration equations in the rotor system. The Lagrange equation is a partial differential equation that understands the balance of forces due to energy in the rotor system. The energy that occurs in a rotor includes rotational kinetic energy, translational kinetic energy, strain energy due to bending moments, strain energy due to axial forces, and energy due to external forces acting on the system [3]. The *previous equation substitutes the T and U* for each rotor element (disk, shaft, unbalance, bearings and seals).

$$\frac{d}{dt}\left(\frac{\partial T}{\partial \dot{q}_i}\right)-\frac{\partial T}{\partial \dot{q}_i}+\frac{\partial U}{\partial \dot{q}_i}=Fq_i \quad (1)$$

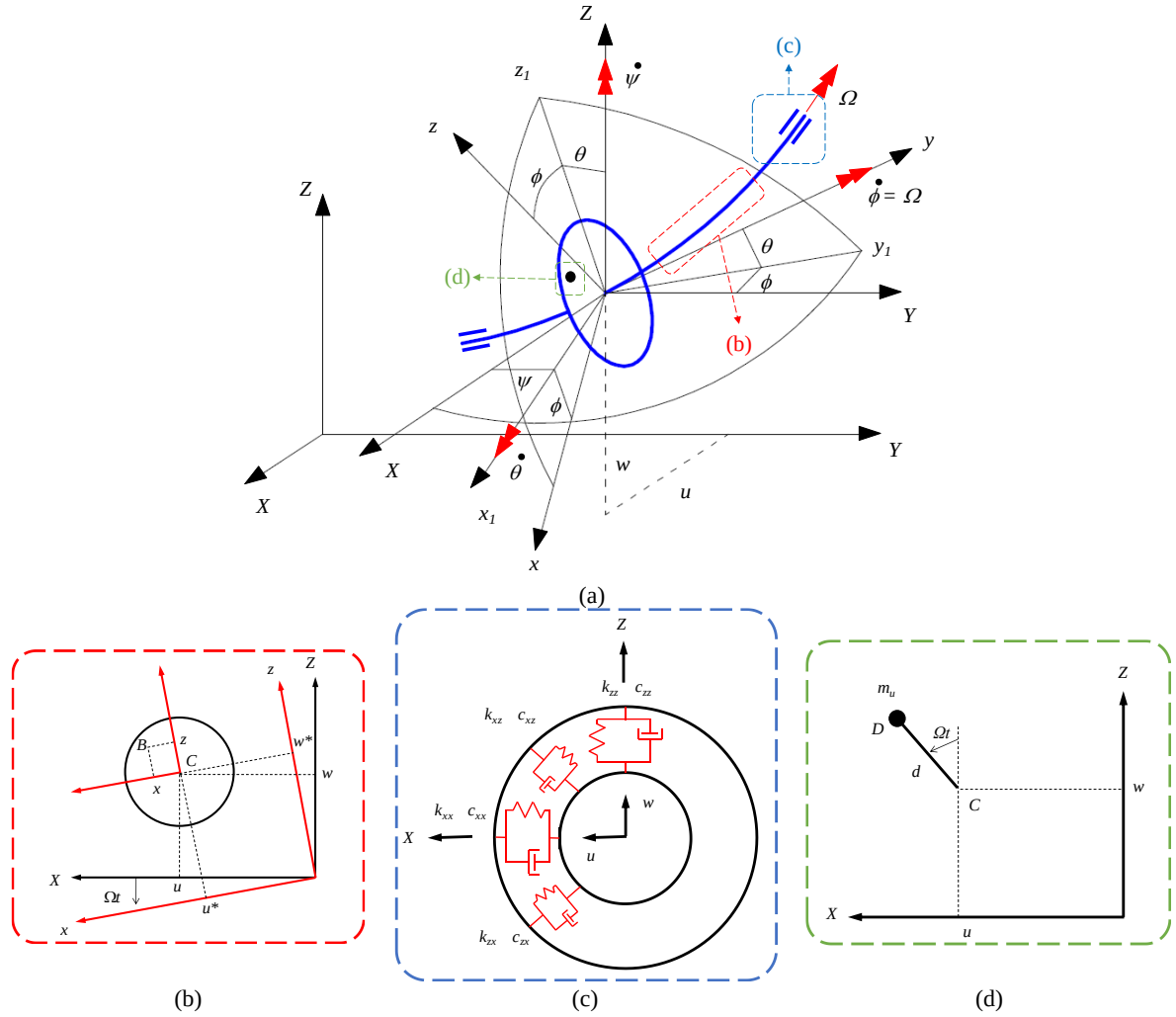

Fig. 5. (a) Schematic of the reference frame for a disk on a flexible shaft; (b) Coordinates of the geometric center C and arbitrary point B on the shaft; (c) Schematic bearings stiffness and damping; (d) Schematic of mass unbalance (Adapted from Lalanne and Ferraris [3])

3. RESULT AND DISCUSSION

3.1. Single Disk Rotor Model

The result for model 1 was conducted by comparing the frequency and critical speed between the FEA and analytical methods. The natural frequency of the model is 44.70 Hz. The natural frequency was obtained when the rotor rotational speed was at zero rpm. The FEA obtained a smaller natural frequency than the references. The comparison to the analytical got a discrepancy of about 2.316%. The comparison to the Ref. [3] and [32] got discrepancies of about 2.325% and 3.325%, respectively. Ref. [3] and [32] have a similar method to the analytical.

Fig. 6 depicts the relationship between the rotor (F) frequency in Hz and rotational speed (*N*) in rpm. The red and blue lines are the frequency line, and the black line is the frequency response line. The red lines describe the phenomena of the forward whirl (FW) phenomena, and the blue lines are for the backward whirl (BW). The intersection point between the frequency line and the frequency response line (F=N/60) obtained the critical speed of the rotor

system. This graph is referred to as the Campbell Diagram. According to the comparison, the result shows a small discrepancy and provides good accuracy to the model. In the FEA, the calculation result depends on the number of element models. The initial model used 3 elements model. The improved model used 6 elements model; the additional elements to investigate the convergence of the result. This model provides a similar effect between initial and enhanced models.

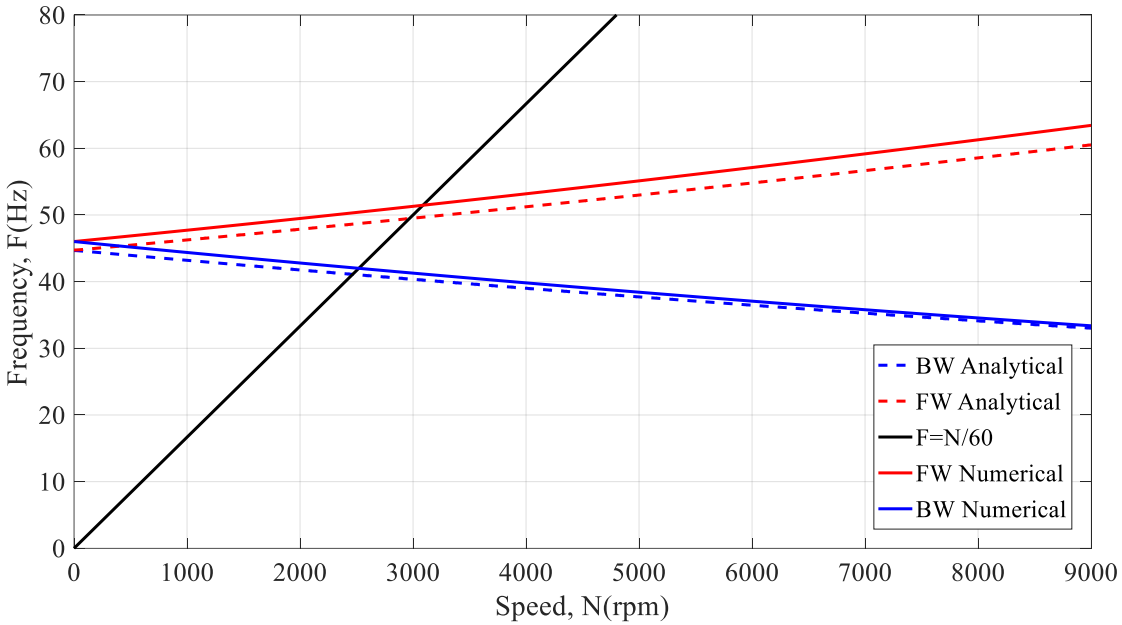

Fig. 6. FEA against analytical method in Campbell diagram for validation model 1

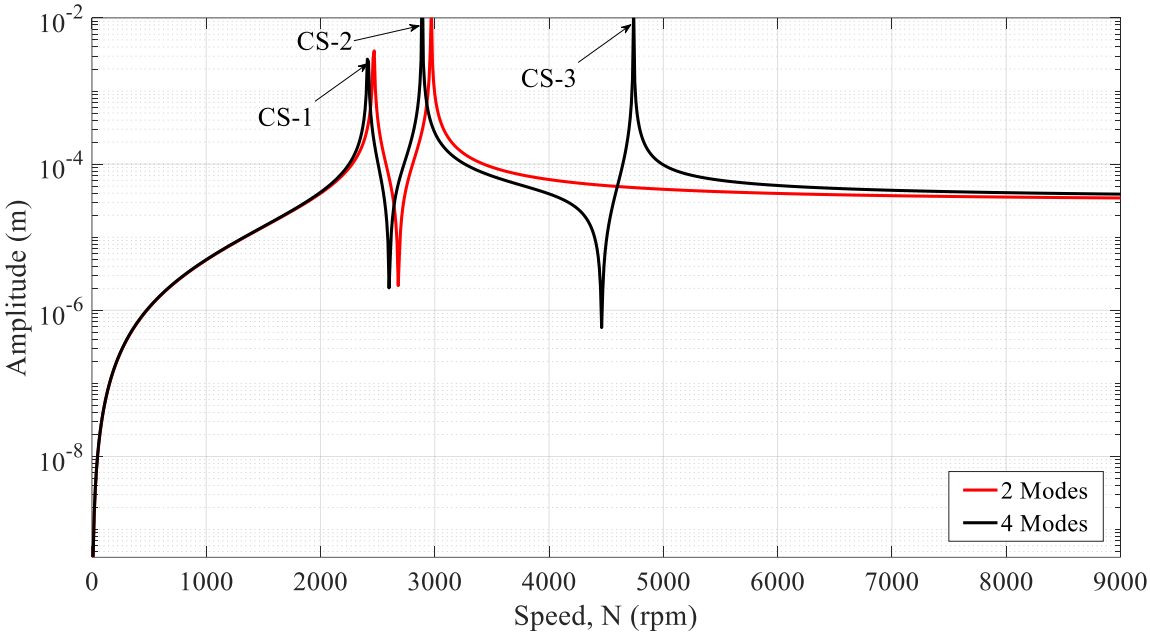

Fig. 7. Mass unbalance response in various modes (2 and 4) for model 1

The intersection solid black line (F=N/60) with red and blue lines shows the peak amplitude at a certain rotational speed. It shows the critical speed which responds due to the mass unbalance. In Fig. 6, the intersection occurred at around 2500 rpm. The response

amplitude is described in Fig. 7. Fig. 7 comprises two analyses. The black line shows the unbalance response in 2 mode shape, and the red line shows the unbalance response in the 4 mode shape. In the range of rotational speed (0-9000 rpm), the peak amplitude occurs at the point of rpm, namely 2500, 3000 and 4800 rpm. In this range, only three peak amplitudes and possibly the fourth peak amplitude occurred out of the range of this operational speed. In this graph, the rotor designer can manipulate the system to avoid peak amplitude at its operational speed. Suppose the best operational speed is between 3000 and 4800 rpm.

Fig. 8 depicts the comparison mass unbalance response in the variety of mass unbalances in g.mm. It shows that the mass unbalance magnitude cannot provide a different result of critical speed. Each mass unbalances different amplitude outside the critical speed region. However, the bigger mass imbalance produces a higher amplitude out of the critical speed range.

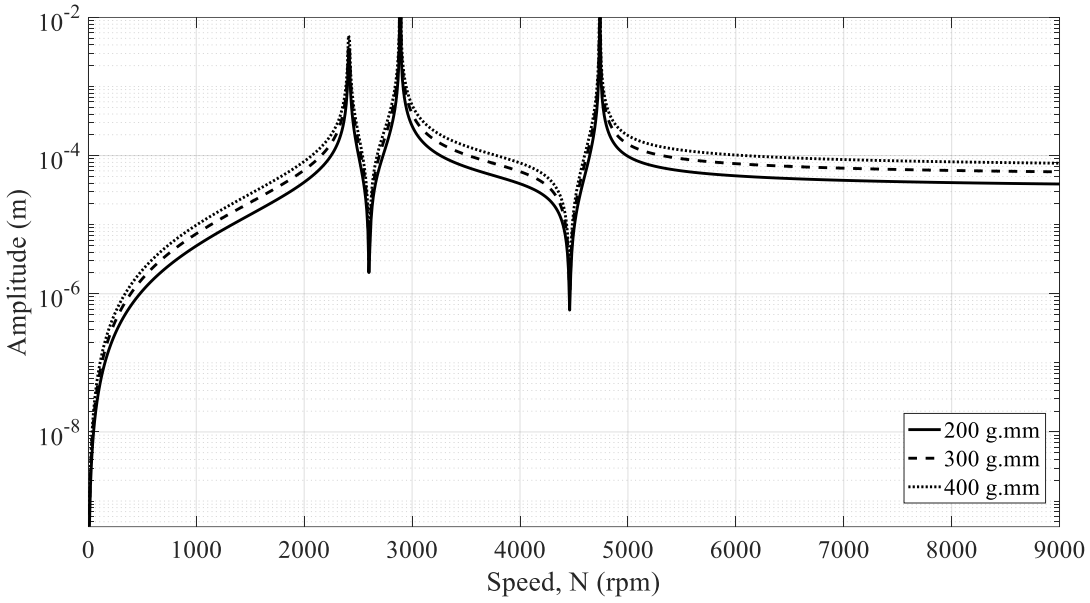

Fig. 8. Mass unbalance response in various mass unbalances (4 mode shape) for model 1

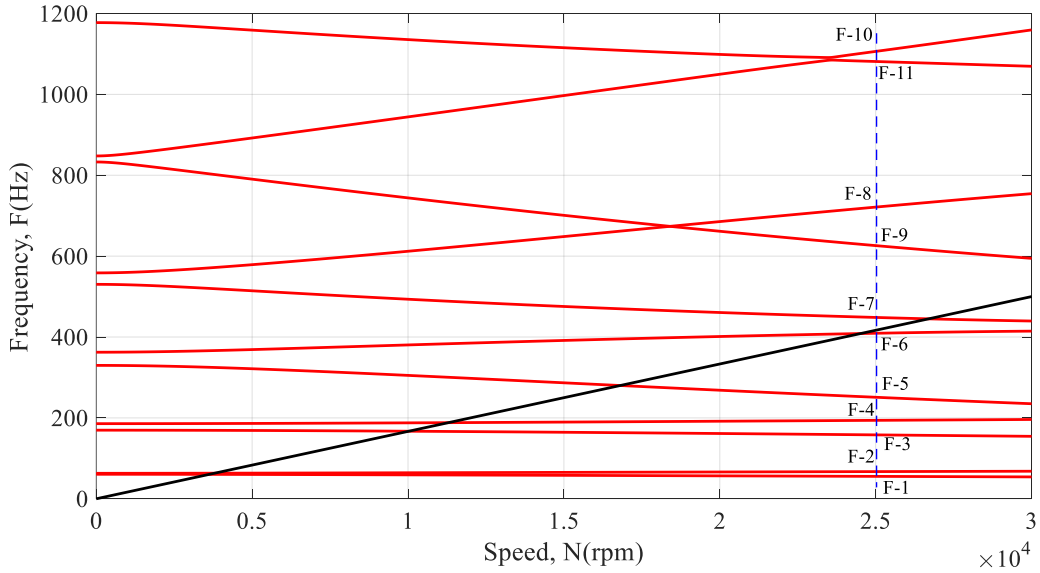

Fig. 9. Campbell diagram for validation model 2

3.1. Multi Disk Rotor Model

The results for model 2 by comparing the frequency and critical speed between the FEA and Ref. [3]. The first natural frequency of the model is 61.84 Hz, which is obtained when the rotor rotational speed is at zero rpm. Fig. 9 shows the relationship between the rotor (F) frequency in Hz unit and rotational speed (*N*) in rpm. The red and blue lines are the frequency line, and the black line is the frequency response line. The red lines describe the phenomena of the forward whirl (FW) and backward whirl (BW) with different orientations. The intersection point between the frequency line and the frequency response line (F=N/60) gets the critical speed of the rotor system.

Table 2 shows the natural frequency for model 2 against the Reference. The result shows a small discrepancy between the model and Reference. The biggest error occurred in F-5 by 1.81%. The average error is 0.67% for 14 modes (10 natural frequencies).

Table 2: Frequencies of the rotor at 25000 rpm (14 modes) for model 2

Frequency	Reference [3] (Hz)	FEA (Hz)	Error (%)
F-1	55.41	55.70	0.53
F-2	67.21	67.07	0.21
F-3	157.90	158.75	0.54
F-4	193.71	193.54	0.09
F-5	249.90	254.43	1.81
F-6	407.62	407.86	0.06
F-7	446.62	450.65	0.90
F-8	715.03	714.26	0.11
F-9	622.65	632.83	1.63
F-10	1093.00	1083.70	0.85

Table 3: Critical of rotor up to 30000 rpm (8 modes)

Critical Speed	Reference [3] (rpm)	FEA (rpm)	Error (%)
CS-1	3620.50	3620.00	0.01
CS-2	3798.30	3800.00	0.04
CS-3	10018.00	10000.00	0.18
CS-4	11281.00	11270.00	0.10
CS-5	16787.00	16880.00	0.55
CS-6	24418.00	24540.00	0.50
CS-7	26611.00	26710.00	0.37

Fig. 10 depicts the mass unbalance response for each mode. Analysis for 2, 4, 6, and 8 modes. In the range of speed (0-30000 rpm), the number of modes shows several critical speeds. It should be a similar number between mode and critical speed. However, eight modes got only 7 critical because the 8th critical speed could occur above 30000 rpm.

The number of critical speeds depends on the number of modes. It shows the prediction of critical speed occurring in the operational speed range. The number of modes shall be considered to know the critical speed at a higher speed. The result of 7 critical speeds (8 modes) compared to Reference is shown in Table 3.

Fig. 11 shows the mass unbalance response in various disks. Although the mass unbalances having different positions due to disk location, the critical speeds occurred in similar positions.

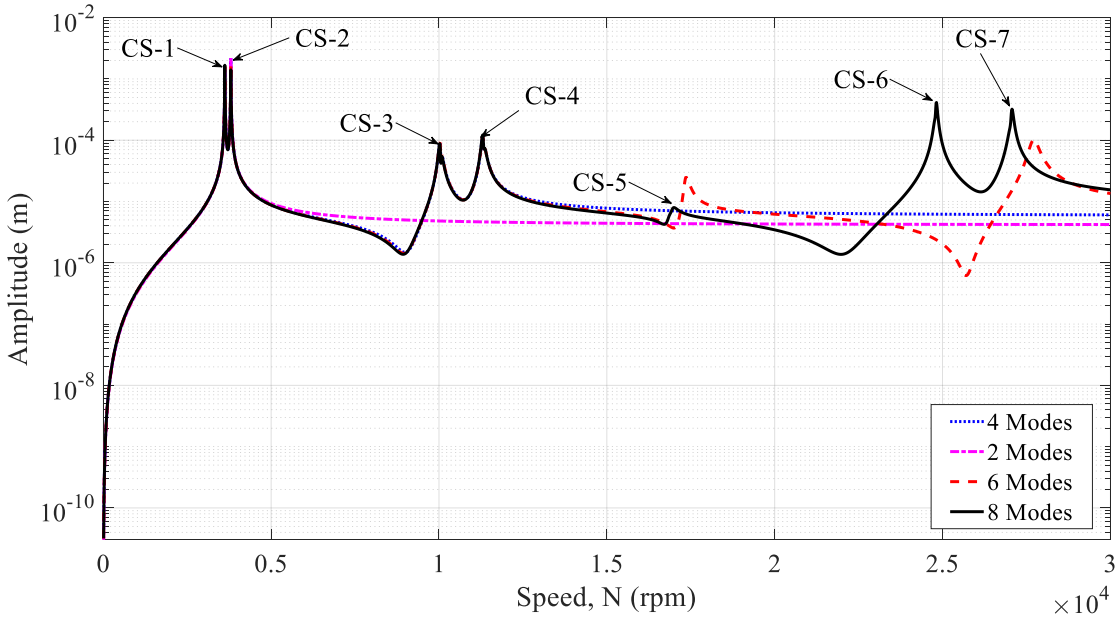

Fig. 10. Mass unbalance response in various modes (2, 4, 6, and 8) for model 2

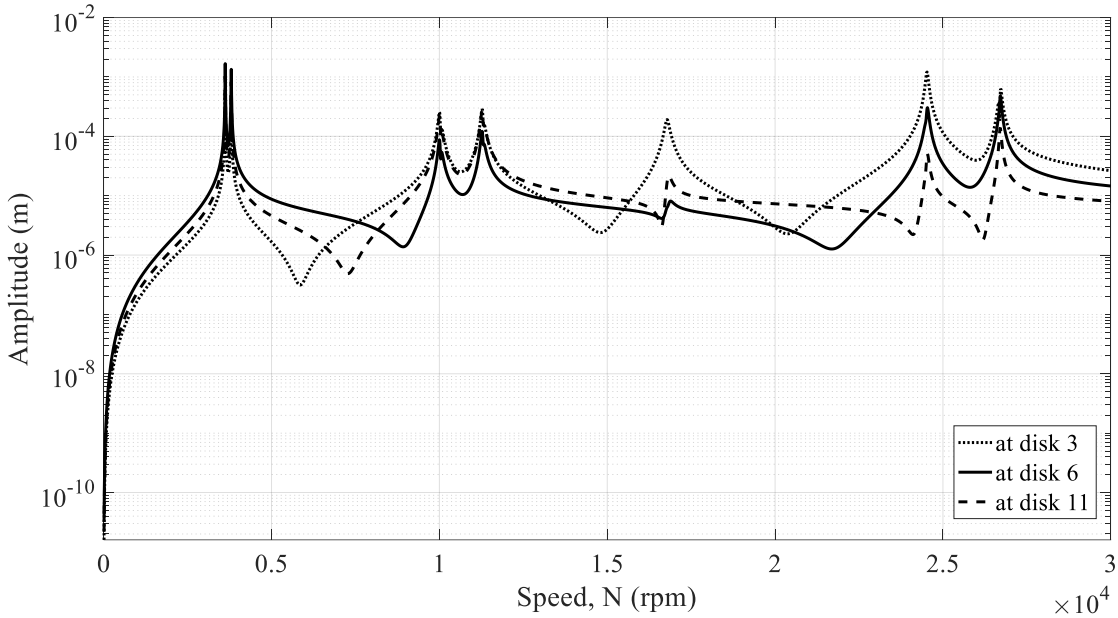

Fig. 11. Mass unbalance response in various positions (at disk 3, 6, and 11)

4. CONCLUSION

The rotordynamic prediction using the FEA program has been conducted for single and multi-disk rotors. Dynamic rotor characteristics can be predicted, such as critical speed and mass unbalance response, where the prediction results with good agreement results and small discrepancies. The development formulation can be created for another case rotor, such as a coaxial dual rotor shaft system. It can be carried out to ensure that the program can predict another type of rotors and that the program can be applied in the general case. The program's implementation with the real case study shall also be conducted to satisfy the assumption taken in the calculation, such as bearing coefficient (stiffness and damping).

ACKNOWLEDGEMENT

We would like to express our deep gratitude to management and Engineering and Technology Division staff for their guidance, encouragement, and useful critiques of this research work.

REFERENCES

[1] O. Matsushita, M. Tanaka, H. Kanki, M. Kobayashi, and P. . Keogh, "Introduction of Rotordynamics," 2017, pp. 1–12.
[2] O. Matsushita, M. Tanaka, M. Kobayashi, P. . Keogh, and H. Kanki, *Vibrations of Rotating Machinery: Volume 2. Advanced Rotordynamics: Applications of Analysis, Troubleshooting and Diagnosis*. 2019.
[3] M. Lalanne and G. Ferraris, *Rotordynamics prediction in engineering* , 2nd ed. Chichester ; John Wiley, 1998.
[4] J. M. Vance, *Rotordynamics of turbomachinery*. John Wiley & Sons, 1991.
[5] L. San Andrés, "Introduction to Pump Rotordynamics," p. 27, Nov. 2006.
[6] M. Sciancalepore, A. Beretta, and H. Satish, *TORSIONAL ROTORDYNAMIC EXCITATION, NATURAL FREQUENCY AND DAMPING CHARACTERISTICS IN A VISCOUS CENTRIFUGAL PUMP APPLICATION*. 2019.
[7] W. Dmochowski, M. Conlon, A. Dadouche, and M. Fillon, "Dynamic Characteristics of Fluid Film Bearings," 2013, p. Vol. 2, pp. 801–808.
[8] J. W. Lund, "Stability and damped critical speeds of a flexible rotor in fluid-film bearings," 1974.
[9] L. San Andre' s and O. De Santiago, "Imbalance response of a rotor supported on flexure pivot tilting pad journal bearings in series with integral squeeze film dampers," *J. Eng. Gas Turbines Power*, vol. 125, no. 4, pp. 1026–1032, 2003.
[10] J. S. Rao, *History of rotating machinery dynamics*, vol. 20. Springer Science & Business Media, 2011.
[11] M. Nässelqvist, "Simulation and characterization of rotordynamic properties for hydropower units." Luleå tekniska universitet, 2009.
[12] M. Karlberg, "Concept evaluation and contact problems in simple rotordynamical systems." Luleå tekniska universitet, 2003.
[13] H. Holzer, "Tabular method for torsional vibration analysis of multiple-rotor shaft systems," *Mach. Des.*, vol. 141, 1922.
[14] S.-T. Choi and S.-Y. Mau, "Dynamic analysis of geared rotor-bearing systems by the transfer matrix method," *J. Mech. Des.*, vol. 123, no. 4, pp. 562–568, 2001.
[15] N. T. Sivaneri and I. Chopra, "Dynamic stability of a rotor blade using finite element analysis," *AIAA J.*, vol. 20, no. 5, pp. 716–723, 1982.
[16] H. D. Nelson and J. M. McVaugh, "The dynamics of rotor-bearing systems using finite elements," 1976.
[17] M. S. Kumar, "Rotor Dynamic Analysis Using ANSYS BT - IUTAM Symposium on Emerging Trends in Rotor Dynamics," 2011, pp. 153–162.
[18] N. Tenali and S. Kadivendi, "Rotor dynamic analysis of steam turbine rotor using ANSYS," *Int. J. Mech. Eng. Robot. Res.*, vol. 1, 2014.
[19] H. Klement, "Program MADYN," 1993, pp. 365–369.
[20] S. Becze and G. Vuscan, "Comparison study regarding bearing performance on 3 types of air bearingsusing Dyrobes software," *MATEC Web Conf.*, vol. 299, p. 4001, Jan. 2019, doi: 10.1051/matecconf/201929904001.
[21] R. Silva *et al.*, "ROSS - Rotordynamic Open Source Software," *J. Open Source Softw.*, vol. 5, p. 2120, Apr. 2020, doi: 10.21105/joss.02120.
[22] A. Hasani, R. Firouz-Abadi, F. Mehralian, M. Rokn-Abadi, M. R. Borhanpanah, and S. Mousavi, *Rotor dynamics analysis of a arbitrary rotor by RoViLab software*. 2021.
[23] H. Taplak and M. Parlak, "Evaluation of gas turbine rotor dynamic analysis using the finite element method," *Measurement*, vol. 45, no. 5, pp. 1089–1097, 2012.

[24] J. J. Moore, G. Vannini, M. Camatti, and P. Bianchi, "Rotordynamic Analysis of a Large Industrial Turbocompressor Including Finite Element Substructure Modeling," *J. Eng. Gas Turbines Power*, vol. 132, no. 8, May 2010, doi: 10.1115/1.2938272.
[25] S. E. Pace, S. Florjancic, and U. Bolleter, "Rotordynamic developments for high speed multistage pumps," 1986.
[26] L. Shuguo, M. Yanhong, Z. Dayi, and H. Jie, "Studies on dynamic characteristics of the joint in the aero-engine rotor system," *Mech. Syst. Signal Process.*, vol. 29, pp. 120–136, 2012, doi: https://doi.org/10.1016/j.ymssp.2011.12.001.
[27] R. S. Mohan, A. Sarkar, and A. S. Sekhar, "Vibration analysis of a steam turbine blade," in *INTER-NOISE and NOISE-CON Congress and Conference Proceedings*, 2014, vol. 249, no. 7, pp. 1055–1064.
[28] T. Hirano, T. Sasaki, H. Sakakida, T. Uchida, M. Tsutsui, and K. Ikeda, "Evaluation of Rotordynamic Stability of a Steam Turbine Due to Labyrinth Seal Force BT - Challenges of Power Engineering and Environment," 2007, pp. 361–367.
[29] J. J. Moore, "Three-Dimensional CFD Rotordynamic Analysis of Gas Labyrinth Seals ," *J. Vib. Acoust.*, vol. 125, no. 4, pp. 427–433, Oct. 2003, doi: 10.1115/1.1615248.
[30] S. Subramanian, A. S. Sekhar, and B. V. S. S. S. Prasad, "Rotordynamic characteristics of rotating labyrinth gas turbine seal with centrifugal growth," *Tribol. Int.*, vol. 97, pp. 349–359, 2016, doi: https://doi.org/10.1016/j.triboint.2016.01.003.
[31] P. Berthier, G. Ferraris, and M. Lalanne, "Prediction of critical speeds, unbalance and nonsynchronous forced response of rotors," in *53rd Symposium on Shock and Vibration. Part 4: Damping and Machinery Dynamics*, 1983, pp. 103–111.
[32] C. W. De Silva, *Vibration and shock handbook*. CRC press, 2005.